American Mineralogist, Volume 74, pages 177–186, 1989

Thermal behavior of complex, tunnel-structure manganese oxides

David L. Bish
Geochemistry and Geology, Mail Stop D469, Los Alamos National Laboratory, Los Alamos, New Mexico 87545, U.S.A.
Jeffrey E. Post
Department of Mineral Sciences, Smithsonian Institution, Washington, D.C. 20560, U.S.A.

Abstract

The manganese oxide minerals coronadite, romanechite, and todorokite occur in a wide range of geologic settings and are common minor phases in massive deposits and as fracture linings. We have studied the thermal behavior of these minerals using a combination of thermogravimetric analysis, differential scanning calorimetry, water analysis, and X-ray powder diffraction. All of these minerals are relatively insensitive to heating up to 400 °C, and the most significant result of heating is reduction of Mn^{4+} with concomitant evolution of oxygen and structural transformation. The total water content of the tunnel-structure manganese oxides is related primarily to the tunnel size and secondarily to the nature of the tunnel cation. Both coronadite and romanechite retain much of their tunnel water to at least 500 °C. Todorokite gradually loses most of its tunnel water below 400 °C. The lower-temperature evolution of water from todorokite as compared with romanechite and coronadite is probably a reflection of the larger, less-filled tunnels in todorokite. Romanechite and todorokite (and perhaps coronadite) appear to contain water in crystallographically well-defined sites, but water evolution does not appear to have a significant structural impact on these minerals. The structural effects of heating romanechite and todorokite up to 300 °C are limited to a minor change in the β angles. Coronadite is not significantly affected until over 600 °C. At higher temperatures, all of these minerals transform to Mn_2O_3 or Mn_3O_4, admixed with other complex oxides in some cases. The relative insensitivity of the todorokite structure to heating strongly supports the now-accepted tunnel structure of todorokite.

Introduction

The tunnel-structure manganese oxide minerals, including hollandites, romanechite, and todorokite, are relatively common in small amounts on the Earth's surface as fracture coatings and in massive deposits. They are also important deep-sea minerals (Burns and Burns, 1977).

These manganese oxide minerals have frameworks composed of edge-shared MnO_6 octahedra with tunnels occupied by water molecules and a variety of cations. Important natural examples of manganese oxides with tunnel structures include hollandite, coronadite, and cryptomelane (2-octahedra × 2-octahedra tunnels containing Ba, Pb, and K, respectively), romanechite (2-octahedra × 3-octahedra tunnels containing Ba), and todorokite (3-octahedra × 3-octahedra tunnels containing Na, Ca, and K; see Giovanoli, 1985a, and Turner and Buseck, 1979, for a general discussion of the structures and this terminology). The details of the structures, particularly the nature of the tunnels and their contents, are neither well known nor universally accepted (see Post et al., 1982; Bish and Post, 1985; Post and Bish, 1988; Turner and Post, 1988). In addition, little data exist demonstrating the effects of heat on these minerals, particularly the evolution of water and other volatiles during heating and the response of the structure to heating. Potter and Rossman (1979) used infrared spectroscopy to aid in identifying the various minerals contained in tetravalent manganese oxides and to determine the nature of the hydrous species in them. They concluded that hollandite minerals contain only a small amount of water and that the water is in crystallographically poorly defined sites. Conversely, they found that romanechite contains water in a single, crystallographically ordered site. Todorokite appeared to have multiple water sites, with some strongly hydrogen-bonded water. They found no evidence for the presence of hydroxide ions in any of these tunnel-structure minerals.

Thermal analysis techniques, such as thermogravimetric analysis (TGA), differential thermal analysis (DTA), and differential scanning calorimetry (DSC), have been the primary methods used in deciphering the nature of the volatile components and the effects of temperature on these manganese oxides. MacKenzie and Berggren (1970) summarized a number of DTA investigations of simple manganese oxides and hydroxides, but they did not examine any complex manganese oxides. They emphasized that in studying these materials, there are inherent difficulties due to the occurrence of Mn in different oxidation states and to the defect structures of many of the phases. Their data

0003–004X/89/0102–0177$02.00

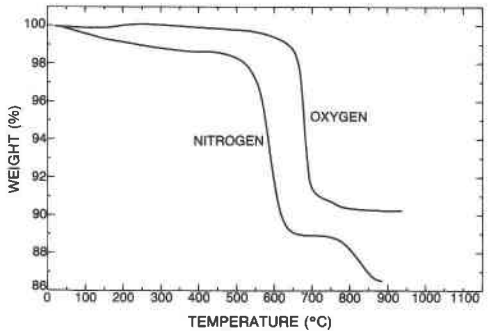

Fig. 1. TGA curves of pyrolusite obtained with N_2 and O_2 purges showing weight loss due to oxygen evolution.

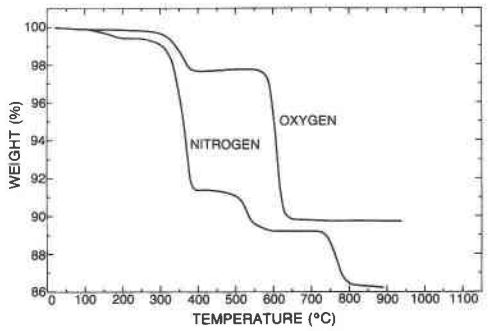

Fig. 2. TGA curves of manganite obtained with N_2 and O_2 purges showing weight losses due to water and oxygen evolution.

on simple manganese oxides and hydroxides show that heating reduces Mn to lower valence states, an effect that generally gives rise to structural changes. For example, pyrolusite (β-MnO_2) transforms to Mn_2O_3 between 625 and 725 °C and then to Mn_3O_4 between 950 and 1050 °C. These transformations are reflected in two discrete weight losses in our N_2-purge TGA data (Fig. 1). Manganite (MnOOH) transforms to Mn_2O_3 at 350–400 °C and to Mn_3O_4 between 900 and 1000 °C (Kulp and Perfetti, 1950). The TGA data for manganite are complicated by the loss of both water and oxygen (Fig. 2). It is implicit in these reactions that oxygen is released as well as water upon heating.

Available data on the complex tunnel-structure manganese oxides containing alkali and alkaline-earth cations are not consistent and in many cases indicate the presence of impurities. Faulring et al. (1960) (and several others referenced therein) used X-ray rotation photographs to examine the structural changes taking place upon heating cryptomelane. They found that the changes were analogous to those occurring with pyrolusite: a transformation from cryptomelane to bixbyite (Mn_2O_3) at about 600 °C, to hausmannite (Mn_3O_4) at about 900 °C, and to a spinel-structure material at higher temperatures or when heated for longer times. However, no phases were identified that could accommodate the 3% to 4% K_2O in the original cryptomelane, although such a phase would likely be present in small amounts. Their TGA data gave a total weight loss of 11.3%, 3.25% due to water and the remaining 8.05% due to oxygen. Coronadite is isostructural with cryptomelane, and the thermal reactions of coronadite should be analogous to those observed for cryptomelane.

MacKenzie and Berggren (1970) presented conflicting data for romanechite (called psilomelane by them). All DTA data presented were featureless below about 700 °C, with several exotherms and endotherms above this temperature for samples from Santiago, Cuba, and from New Mexico. Wadsley (1950) found that synthetic romanechite (called psilomelane) transformed to hollandite when heated to 550 °C, in agreement with Fleischer and Richmond (1943). In fact, Wadsley (1950) considered romanechite a necessary phase in the paragenesis of hollandite because of the relative ease with which romanechite transforms to hollandite. On the basis of DTA data, Kulp and Perfetti (1950) concluded that, although no low-temperature reactions occur with romanechite, a characteristic exothermic recrystallization reaction occurs between 800 and 1000 °C. However, they recognized the problem of impurities and emphasized that study of the complex manganese oxides such as romanechite is unwarranted in the absence of other confirming data such as chemical analyses, noting the presence of pyrolusite in one of their romanechite (psilomelane) samples. Giovanoli (1985a) examined the thermal behavior of a synthetic romanechite and concluded that water is released continuously on heating and that a gradual transformation to hollandite takes place as the tunnels collapse around the Ba cations. In addition, mass spectrometric analysis of evolved gases while heating showed that water is given off at low temperatures and that oxygen evolution peaks at about 690 °C. The end products of heating their romanechite in a vacuum above 800 °C were Mn_3O_4 and $BaMnO_3$.

Straczek et al. (1960) presented, but did not interpret, a differential thermal analysis curve of todorokite from the Quinto Pit, Cuba. Recently, Dubrawski and Ostwald (1987) examined a very poorly ordered marine todorokite by DSC, TGA, and X-ray diffraction methods. They appear to have considered that all of the weight loss seen with the TGA was due to water and neglected the effects of Mn reduction and oxygen evolution. The higher-temperature phases of todorokite were "substituted hausmannite" and Mn_2O_3. To our knowledge, there are no other data on the thermal behavior of well-characterized todorokite. Thermal data on layer-structure manganese oxides such as birnessite are not considered here, and the interested reader is referred to Giovanoli (1985a), Chen et al. (1986), Golden et al. (1986, 1987), and Dubrawski and Ostwald (1987).

We have examined the thermal behavior of well-characterized, relatively pure samples of coronadite, romanechite, and todorokite, representatives of 2 × 2, 2 × 3, and 3 × 3 tunnel structures, respectively, using TGA, water analysis, and high-temperature XRD (Bish and Post, 1984). These experiments were not plagued by the usual problems of impurities and have provided insight into the

TABLE 1. Sources and chemical formulae of manganese oxides used in this study

Sample	Locality	Formula
Pyrolusite, HU 111929	Lake Valley, New Mexico	MnO_2*
Manganite, 83837	Hartz Mountains, Germany	MnOOH (assumed)
Coronadite, HU 106257	Broken Hill, Australia	$Pb_{1.4}(Mn^{4+},Mn^{3+})_8O_{16}\cdot 1.55H_2O$*† (approximate)
Hollandite, USNM 127118	Stuor Njuoskes, Sweden	$Ba_{0.75}Pb_{0.16}Na_{0.10}(Mn^{3+},Mn^{4+})_{6.56}Fe^{3+}_{1.32}Al_{0.23}O_{16}\cdot 0.79H_2O$*†
Cryptomelane, USNM 89104	Chindwara, India	$K_{0.94}Na_{0.25}Sr_{0.13}Ba_{0.10}(Mn^{3+},Mn^{4+})_{7.53}Fe^{3+}_{0.3}Al_{0.15}O_{16}\cdot 0.3H_2O$*†
Romanechite, HU 97618	Van Horne, Texas	$Ba_{0.52}Na_{0.06}Ca_{0.05}K_{0.04}(Mn^{3+},Mn^{4+})_{4.92}Mg_{0.06}O_{10}\cdot 1.3H_2O$*†
Romanechite, USNM C1818	Schneeburg, Germany	$Ba_{0.66}Ca_{0.03}Na_{0.01}(Mn^{4+},Mn^{3+})_{4.81}O_{10}\cdot 1.3H_2O$*†
Todorokite, HU 126232	N'Chwaning mine, South Africa	$Na_{0.40}Ca_{0.14}K_{0.01}(Mn^{4+},Mn^{3+})_{5.61}Mg_{0.43}O_{12}\cdot 4.59H_2O$*†
Todorokite	Hotazel, South Africa	Similar to no. 126232
Todorokite, HU 106783	Farragudo, Portugal	$Na_{0.27}K_{0.18}Ca_{0.05}(Mn^{4+},Mn^{3+})_{5.64}Mg_{0.36}O_{12}\cdot 4.0H_2O$*†
Todorokite, HU 106238	Charco Redondo, Cuba	$Na_{0.26}Ca_{0.22}K_{0.03}Sr_{0.03}Ba_{0.01}(Mn^{4+},Mn^{3+})_{5.54}Mg_{0.45}O_{12}\cdot 3.81H_2O$†‡
	Ba-exchanged	$Na_{0.25}Ca_{0.18}K_{0.03}Sr_{0.03}Ba_{0.05}(Mn^{4+},Mn^{3+})_{5.55}Mg_{0.45}O_{12}\cdot 3.89H_2O$†‡
	Sr-exchanged	$Na_{0.25}Ca_{0.19}K_{0.03}Sr_{0.06}Ba_{0.01}(Mn^{4+},Mn^{3+})_{5.52}Mg_{0.44}O_{12}\cdot 3.77H_2O$†‡

Note: HU = Harvard University Museum; USNM = U.S. National Museum.
* Microprobe analysis.
† Water from DuPont MEA.
‡ Atomic absorption analysis.

structural changes taking place upon heating and into the nature of tunnel water molecules. In addition, our experiments provide some insight into the structure of todorokite.

Experimental details

To ensure purity before conducting thermal studies, we examined all samples by X-ray powder diffraction using a Siemens D-500 diffractometer with Cu$K\alpha$ radiation and a graphite monochromator. Samples studied (Table 1) included todorokite from Charco Redondo, Cuba, from Farragudo, Portugal, from Hotazel, South Africa, and from the N'Chwaning mine, North Cape Province, South Africa; romanechite from Van Horne, Texas, and from Schneeburg, Germany; and coronadite from Broken Hill, Australia. In addition, Ba- and Sr-exchanged samples of the Cuban todorokite, prepared by suspending the todorokite in 0.5 *M* solutions of the chlorides for one week, were examined to assess the effects of tunnel-cation composition on thermal behavior and water content (Bish and Post, in prep.). For comparison purposes, we also examined a sample of pyrolusite from Lake Valley, New Mexico, admixed with minor ramsdellite, and a manganite sample from the Hartz Mountains, Germany. Finally, to shed light on the manner in which 2 × 2 tunnel structures lost water, we studied samples of hollandite from Stuor Njuoskes, Sweden, and cryptomelane from Chindwara, India, both previously examined by Post et al. (1982). Chemical formulae were obtained by both electron-microprobe and atomic-absorption methods, and amounts of water were obtained with a DuPont moisture evolution analyzer (MEA). X-ray data for romanechite and coronadite are in Post and Bish (in prep.), and data for the todorokite samples are given in Post and Bish (1988).

To monitor the reactions occurring on heating, we examined romanechite and todorokite at 50 °C intervals up to 300 °C in a vacuum (10^{-1} torr) in an Anton Paar heating stage on the Siemens X-ray diffractometer. The upper temperature limit for the heater is 300 °C, and the stage must be evacuated above 200 °C. We were thus able to quantify the *d*-spacing and intensity changes that accompanied loss of water and oxygen. Unit-cell parameters were obtained up to 300 °C using the least-squares refinement program of Appleman and Evans (1973). In addition to the data obtained at higher temperatures, X-ray diffraction patterns were obtained at room temperature for samples of coronadite, romanechite, and todorokite after heating in air at temperatures up to 1000 °C in 100 °C intervals for ~15 h.

For TGA and DSC analyses, we used a DuPont 1090 system with a model 951 TGA and 910 DSC. Experiments were conducted in dynamic N_2 and O_2 atmospheres with sample sizes of generally 10 to 15 mg and a heating rate of 10 °C/min. For most of the manganese oxides listed in Table 1, we determined total water content and evolution of water during heating with a DuPont 903H MEA on 10- to 20-mg samples in a dry N_2 atmosphere. These water analyses provided valuable additional information because TGA data are complicated by the simultaneous evolution of water and oxygen with heating, giving rise to weight losses significantly greater than would be expected solely from the loss of water.

Results

As noted above, all samples yielded weight losses in the TGA considerably greater than would be expected from water loss only. The TGA data for pyrolusite (MnO_2) (Fig. 1) and manganite (MnOOH) (Fig. 2) clearly illustrate this effect. After an initial minor low-temperature weight loss probably due to adsorbed water, pyrolusite undergoes two major weight losses. The first, occurring between 500 and 600 °C in N_2, corresponds to the reaction $2MnO_2 \rightarrow Mn_2O_3 + 0.5O_{2(g)}$. The observed weight loss of 9.7% agrees closely with the theoretical value of 9.2%. The second weight loss, occurring above 750 °C, corresponds to the reduction reaction $3Mn_2O_3 \rightarrow 2Mn_3O_4 + 0.5O_{2(g)}$ (3.07% theoretical, ~2.5% observed). This reduction reaction was not complete at the highest temperature reached in this experiment, accounting for the relatively low observed weight loss. The temperature range of the first reaction is

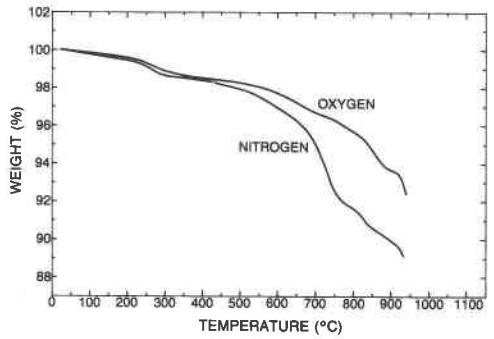

Fig. 3. TGA curves of coronadite obtained with N_2 and O_2 purges.

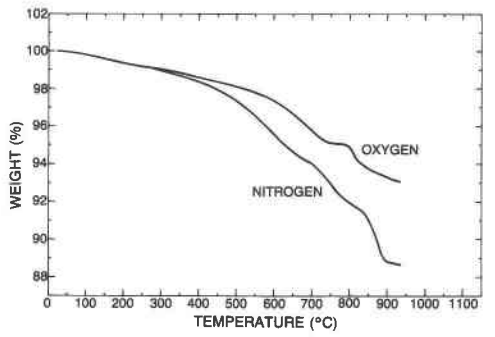

Fig. 4. TGA curves of Van Horne romanechite obtained with N_2 and O_2 purges.

elevated by about 100 °C in an oxygen atmosphere, and the second reaction is not evident at the highest temperature in the oxygen atmosphere, illustrating the dramatic effect of purge gas on oxygen loss. Manganite undergoes both a dehydration reaction, $2MnOOH \rightarrow Mn_2O_3 + H_2O_{(g)}$ (10.2% theoretical), and a reduction reaction, $3Mn_2O_3 \rightarrow 2Mn_3O_4 + 0.5O_{2(g)}$ (3.0% theoretical). The TGA data in Figure 2 reveal a complex thermal behavior, with at least three distinct weight losses in a N_2 atmosphere and two in oxygen. The total weight loss in N_2 is 13.76%, slightly greater than the theoretical loss. The greater weight loss may be due to adsorbed water or to the presence of some Mn^{4+} in the manganite; moisture evolution analysis yielded a total water content of 11.46% compared with 10.2% theoretical. We have not determined if the total weight loss is a function of particle size. Both Figure 1 and Figure 2 illustrate that the thermal behavior of even simple manganese oxides is relatively complex, and it is obvious that the TGA data are dominated by a loss of oxygen during reduction of higher oxidation states of Mn.

The TGA data for coronadite (Fig. 3) reveal several gradual losses in weight primarily associated with a loss of oxygen. The TGA data for all manganese oxides can be elucidated through comparison of oxygen- and N_2-purge TGA data and by comparison of TGA data with MEA data measured at discrete intervals (Table 2). The effect of changing from a N_2 purge to an oxygen purge for coronadite is to shift all but the lowest-temperature (275 °C) weight loss to higher temperatures, suggesting that much of the 1.5% weight loss occurring up to about 275 °C is due to water. Divergence of the two TGA curves suggests that significant oxygen evolution does not begin until about 400 °C. At higher temperatures, several gradual weight losses are apparent, resulting in a total weight loss in excess of 11%. The MEA data reveal that the most significant water loss is between 300 and 600 °C. This largest water loss began at about 230 °C during the MEA measurement as shown by increased count rate when the MEA temperature exceeded 230 °C on the way to 300 °C. The thermal reactions of coronadite are dominated by Mn reduction, and water plays a minor role in this 2 × 2 tunnel-structure mineral. MEA data on two other 2 × 2 manganese oxide minerals, hollandite and cryptomelane, reveal similar low water contents, with peak water evolution occurring between 600 and 800 °C (Table 2).

The TGA data for romanechites are similar to those for coronadite, and data for the Van Horne, Texas, romanechite (Fig. 4) show several gradual, overlapping weight losses. Data collected in an oxygen atmosphere show similar transitions shifted about 200 °C up in temperature. Comparison of MEA and TGA data for the Van Horne, Texas, romanechite suggests that oxygen evolution begins at about 300 °C. At that temperature, the two TGA curves begin to diverge. The MEA data (Table 3) reveal a greater water loss at low temperatures (by about 300 °C) than do the TGA data, probably because the MEA measurement is static whereas the TGA measurement is dynamic. However, the total water content determined by MEA is exceeded by the cumulative TGA weight loss occurring up

TABLE 2. Water evolution (wt%) as a function of temperature for coronadite, hollandite, and cryptomelane

T (°C)	No. 106257	No. 127118	T (°C)	No. 89104
100	0.10	0.05	100	0.06
300	0.72	0.14	250	0.12
600	1.66	0.50	400	0.10
800	0.24	0.93	600	0.10
1000	0.03	0.10	800	0.25
			1000	0.08
Total	2.75	1.72		0.71

TABLE 3. Water evolution (wt%) as a function of temperature from two romanechites

T (°C)	No. 97618	No. C1818
100	0.30	0.36
200	0.44	0.52
300	0.66	0.71
400	0.91	0.95
600	2.70	2.21
800	0.14	0.48
1000	0.02	0.10
Total	5.17	5.33

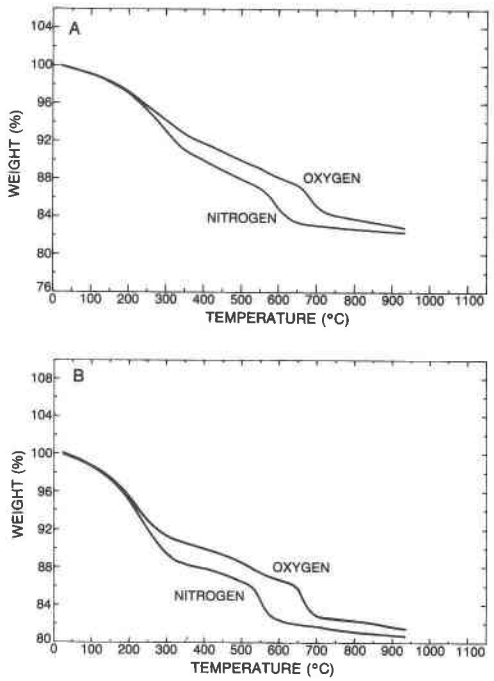

Fig. 5. TGA curves of (**A**) Cuban todorokite and (**B**) Portuguese todorokite obtained with N_2 and O_2 purges.

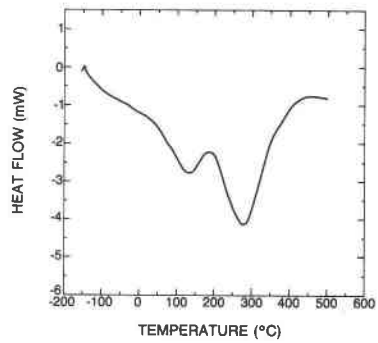

Fig. 6. DSC curve of Portuguese todorokite obtained with a N_2 purge.

to 650 °C. The MEA data for both romanechites reveal a gradual loss of water, peaking between 400 and 600 °C. The TGA data show that in a N_2 atmosphere, an additional 7 wt% is lost because of oxygen evolution. Oxygen evolution is significantly suppressed in an oxygen atmosphere, and only an additional 2 wt% is lost in the oxygen-purge TGA experiment over the weight loss that can be attributed to water.

The TGA data for todorokites (Figs. 5A, 5B) are similar to those obtained for the other manganese oxides, with a gradual loss in weight up to 950 °C. In addition, the TGA curves show an abrupt weight loss at ~550 °C in a N_2 atmosphere and at ~665 °C in an oxygen atmosphere, probably attributable to the occurrence of a significant structural transformation. The MEA data (Tables 4 and 5) show that most of the water in todorokite is gone by the temperature of this structural transformation. Water evolution is greatest between 100 and 300 °C, with significant amounts held up to 400 °C. Total water contents for the todorokites analyzed range between 11.7% and 13.6%, whereas total weight losses in TGA experiments often exceed 20 wt%. Divergence of the oxygen- and N_2-purge TGA data suggests that oxygen evolution begins around 200 °C, with total oxygen losses of 8 to 10 wt% in N_2-purge TGA experiments. The MEA data for the Ba- and Sr-exchanged todorokites (Table 5) reveal total water contents similar to the unexchanged material and a greater proportion of water held to higher temperatures. The DSC data for todorokite (Fig. 6) reveal two significant endotherms centered at about 130 and 275 °C. These endotherms are undoubtedly associated with the loss of tunnel water; the higher-temperature reactions of todorokite occur above the range of our DSC instrument.

The effects of water loss and Mn reduction leading to oxygen evolution can be clarified up to 300 °C using XRD data collected at various temperatures in the heating stage. Data collected for the Van Horne, Texas, romanechite show that the structure is not greatly affected by heating to 300 °C in a vacuum (Fig. 7). The only "significant" difference in cell parameters between 20 and 300 °C is a decrease in β from 92.15(9)° to 91.96(8)°. The diffraction patterns are virtually identical in peak position and intensity, and the *a, b,* and *c* cell parameters are statistically equivalent throughout the temperature range of the experiment. High-temperature XRD data for the Hotazel, South Africa, todorokite with a Si internal standard reveal more significant changes. The diffraction patterns of the sample at 20 and 300 °C (Fig. 8) are quite different, and the intensities of the todorokite reflections at 300 °C are about half what they are at room temperature. The

TABLE 4. Water evolution (wt%) as a function of temperature for three todorokites

T (°C)	No. 106238	No. 106783	No. 126232
100	1.06	1.64	1.99
200	3.82	5.16	3.47
300	4.76	4.07	6.18
400	1.70	0.58	0.76
600	0.24	0.19	0.50
800	0.06	0.04	0.24
1000	0.09	0.04	0.43
Total	11.73	11.72	13.57

TABLE 5. Water evolution (wt%) as a function of temperature for Ba- and Sr-exchanged todorokite, no. 106238

T (°C)	Ba	Sr
100	0.87	0.90
200	2.94	2.69
300	6.06	4.66
400	1.57	2.68
600	0.25	0.65
800	0.03	0.06
1000	0.08	0.03
Total	11.80	11.67

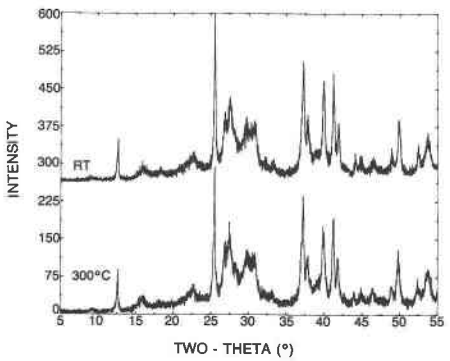

Fig. 7. X-ray diffraction patterns of Van Horne romanechite measured at room temperature (RT) and at 300 °C (both in vacuo) in the heating stage.

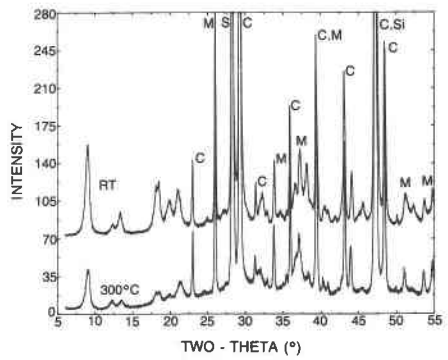

Fig. 8. X-ray diffraction patterns of South African todorokite [with Si (S), calcite (C), and manganite (M)] measured at room temperature (RT) and at 300 °C (both in vacuo) showing the marked decrease in intensity at 300 °C.

intensities of todorokite reflections begin to drop significantly above 150 °C and drop most between 250 and 300 °C. To minimize contamination of limited samples, no other samples were mixed with a Si internal standard. Similar data for the Cuban todorokite reveal a gradual drop in intensity beginning at 100 °C, with a significant reduction beginning at 200 °C. Intensities at 300 °C are about 55% of what they are at room temperature. In addition to the reductions in diffracted intensity, the todorokite unit-cell changes are similar to those noted for romanechite. The a and c parameters for the South African todorokite experience a minor reduction, and the β angle increases significantly, particularly between 250 and 300 °C (Table 6). These data correlate well with TGA and DSC data that reveal a significant transition related to water evolution at about 275 °C.

The XRD data obtained by examining samples heated in a furnace reveal the structural nature of the transformations occurring at higher temperatures. These data (Fig. 9) show that coronadite is relatively unaffected by heating to 600 °C and that a transformation occurs between 700 and 800 °C, correlating well with the point of most rapid weight loss in the N_2-purge TGA data. Coronadite heated to 800 °C yields a complex diffraction pattern, with contributions from $Pb_{0.25}MnO_{1.99}$ (JCPDS no. 36-842), bixbyite (Mn_2O_3), and Pb oxides (JCPDS no. 36-725 and perhaps no. 27-1200). An unidentified phase occurs with a reflection at 11.6 Å, perhaps a superstructure of a Pb-Mn phase. At higher temperatures, bixbyite is the predominant phase, with lesser amounts of other phases identified at 800 °C.

TABLE 6. Cell parameters of South African todorokite as a function of temperature in a 10^{-1} torr vacuum

T (°C)	a (Å)	c (Å)	β (°)
20	9.78(1)	9.58(1)	94.5(1)
50	9.77(1)	9.58(1)	94.5(1)
100	9.75(1)	9.59(1)	94.5(1)
150	9.73(1)	9.57(1)	94.6(1)
200	9.72(1)	9.58(1)	94.6(1)
250	9.77(1)	9.55(1)	94.8(1)
300	9.76(1)	9.56(1)	95.5(1)

Note: The b parameter did not change significantly.

The romanechite structure is largely destroyed between 400 and 500 °C, yielding a "protohollandite" material with only a few broad reflections (Fig. 10). The breakdown of the 2 × 3 tunnel structure between 400 and 500 °C corresponds with the maximum evolution of water between 400 and 600 °C. The material heated to 800 °C consists predominantly of a hollandite-structure phase and Mn_2O_3, and above 800 °C, the material contains predominantly hausmannite (Mn_3O_4) with lesser amounts of the hollandite-structure phase.

In agreement with the heating-stage data, the diffraction patterns for heated Cuban todorokite experience a significant reduction in intensity above 200 °C. This reduction continues through 500 °C, with the basic todorokite diffraction pattern remaining (Fig. 11). Hausmannite, Mn_3O_4, with a unit cell slightly smaller than the end-member Mn phase [a = 5.7459(2) Å and c = 9.4097(6) Å versus a = 5.762 Å and c = 9.4097 Å for pure hausmannite, JCPDS no. 24-734], begins growing at the expense of todorokite by 600 °C, and it is the predominant phase at and above 700 °C, with evidence for todorokite virtually gone by 700 °C. The appearance of hausmannite around 600 °C is consistent with TGA data showing an abrupt weight loss culminating near 600 °C. The decrease in the hausmannite cell size is probably due to substitution of minor Mg or other common impurities for Mn. Contrary to Dubrawski and Ostwald (1987), we saw no evidence for the existence of any form of Mn_2O_3, nor would Mn_2O_3 be expected after the appearance of Mn_3O_4. However, several very broad reflections are apparent in the diffraction pattern of the material heated to 800 °C. These can be seen in Figure 11 at ~19.2°, ~33.4°, and ~37.0° 2θ and are associated with the crystallization of $Na_4Mn_9O_{18}$ (JCPDS no. 27-750), a phase that can accommodate the Na, Ca, and K tunnel cations from the original todorokite. Hausmannite and $Na_4Mn_9O_{18}$ are the only phases obvious after heating to 900 °C, but $Na_4Mn_9O_{18}$ has decreased significantly after heating to

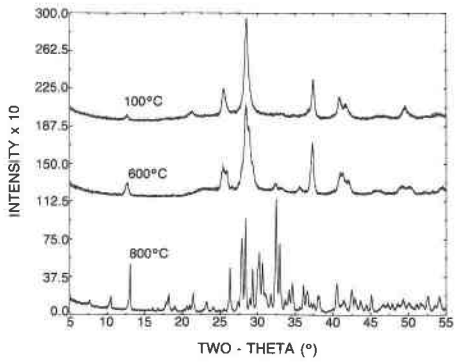

Fig. 9. X-ray diffraction patterns of coronadite measured at room temperature after heating to 100, 600, and 800 °C.

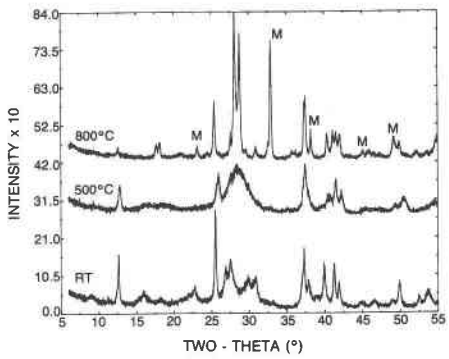

Fig. 10. X-ray diffraction patterns of Van Horne romanechite at room temperature (RT) and after heating to 500 and 800 °C, showing the nucleation of a hollandite-like phase at 500 °C (all data measured at room temperature). Reflections labelled M in the 800 °C pattern are due to Mn_2O_3; unlabeled reflections are due to the hollandite-like phase.

1000 °C, perhaps because of volatilization or migration of Na into the porcelain crucible.

Discussion

Our thermal data show clearly that the primary effect of heating manganese oxide minerals, particularly Mn^{4+}-containing minerals, is reduction of the Mn to lower oxidation states with concomitant evolution of oxygen and structural rearrangement. All of the manganese oxides examined transform to either Mn_2O_3 or Mn_3O_4, sometimes together with more complex oxides. The TGA data for all minerals examined show that oxygen is lost in a stepwise manner in association with transformations to phases containing more reduced Mn. Divergence between N_2-purge and oxygen-purge TGA data suggests that oxygen is evolved from the tunnel-structure minerals during a TGA experiment at temperatures perhaps as low as 200 °C. When the dynamic nature of the TGA experiments is considered, it is possible that the lower limit of oxygen evolution may be significantly below 200 °C under equilibrium conditions. Because of the combined evolution of water and oxygen, it is difficult to obtain complete time- and temperature-resolved data on their evolution.

Thermal data show that coronadite is insensitive to heating up to 600 °C, although a small (<3%) weight loss primarily due to water occurs up to this temperature. Mn_2O_3 is one of the high-temperature transformation products, but we did not observe thermal transformations like those observed by Faulring et al. (1960) for cryptomelane. It is probable that the much greater amount of reduced Mn required by the presence of the divalent tunnel cations in the original coronadite and the larger tunnel occupancy in coronadite (1.4 Pb cations vs. 0.7–0.8 cations, mainly K, for the cryptomelanes studied by Faulring et al.) may be responsible for the different thermal behavior. Although we did not obtain X-ray diffraction data at various temperatures for coronadite using the heating stage, it is likely that the coronadite structure is relatively insensitive to evolution of the water contained in the small 2 × 2 tunnels.

The major structural effect of water evolution in romanechite is a minor change in the β angle, and it appears that evolution of water from romanechite is controlled by the structural transformations resulting from Mn reduction, not vice versa. This cause-effect relationship could be verified by measuring water evolution in the MEA using oxygen as a carrier gas. Because oxygen evolution and presumably the structural transformations that arise from or cause the loss of oxygen are shifted to higher temperatures in an oxygen atmosphere, water evolution would similarly be expected to occur at higher temperatures if it were controlled by the transformations. Unfortunately, operation of the MEA in an oxygen atmosphere is not recommended by the manufacturer. The high-temperature retention of water in romanechite is surprising, particularly in light of the conclusions of Potter and Rossman (1979) that none of these minerals contains significant hydroxyl. The retention of most of the water in romanechite up to 500 °C may be due to the smaller and more-filled tunnels, which restrict the diffusion of water. However, water retention may also be a reflection of the

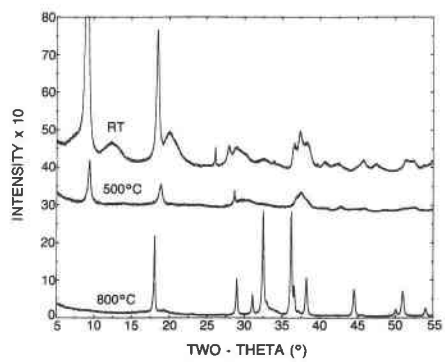

Fig. 11. X-ray diffraction patterns of Cuban todorokite at room temperature (RT) and after heating to 500 and 800 °C (all data measured at room temperature). All sharp reflections in the 800 °C pattern are due to hausmannite, and the very broad reflections are due to $Na_4Mn_9O_{18}$.

occurrence of water in well-defined sites (Potter and Rossman, 1979; Turner and Post, 1988). Conversely, most water is lost from todorokite below 400 °C, before the structure has completely broken down. The major effect of water evolution from both romanechite and todorokite is a minor change in the β angle as the tunnels lose their water. Water molecules apparently play a minor role in propping open the tunnels in both romanechite and todorokite, at least at higher temperatures. The lower-temperature evolution of water from todorokite is probably a reflection of the larger and less-filled tunnels relative to romanechite.

X-ray data suggest that the smaller tunnels in coronadite are more stable than the 2 × 3 and 3 × 3 tunnels in romanechite and todorokite, respectively. In fact, based on the samples we have examined, hollandite-structure material appears to be an intermediate phase in the heating of tunnel-structure manganese oxides with significantly more than 0.5 tunnel cations per 12 oxygens. The primary result of heating these minerals below 500 °C is a small but significant change in the β angle, perhaps as a consequence of water loss. However, the higher-temperature reactions appear to be a result of Mn^{4+} reduction. Although both coronadite and romanechite undergo transitions to Mn_2O_3, todorokite transforms directly to Mn_3O_4, bypassing Mn_2O_3. This transformation sequence, coupled with the loss of considerably less oxygen than expected during the reaction to Mn_3O_4 (~8.3% compared with 12.3% ideal), suggests that natural todorokites may contain a significant proportion of reduced Mn species in addition to minor Mg and Al.

As noted above, the structural details of coronadite and todorokite, and in particular the nature of the tunnel occupants in these minerals, are not well known. The structure of coronadite is analogous to that of hollandite, with the Ba tunnel cation in hollandite replaced by Pb in coronadite (Gruner, 1943; Post et al., 1982). Post et al. (1982) found evidence for a small amount of water at the Ba tunnel-cation sites in hollandite, but they found no evidence for molecular water in cryptomelane. Their difference-Fourier maps for both hollandite and cryptomelane suggested that some of the oxygen atoms in the framework may be hydroxyls. Contrary to this, Potter and Rossman (1979) found no evidence for hydroxyl ions in any of the manganese oxides they examined, and they concluded that the water in hollandite minerals is in poorly defined sites. Our MEA data for hollandite minerals, showing a small amount of water released at relatively high temperatures, are similar to our results for romanechite and do not support the conclusions of Potter and Rossman (1979). It is difficult to imagine weakly bonded water molecules remaining in these tunnel-structure minerals at temperatures over 600 °C. These data also illustrate the significant effect of the tunnel cation on total water contents. Cryptomelane, with predominantly univalent, low-hydration-energy tunnel cations, has considerably less water than hollandite or coronadite, both with divalent tunnel cations.

Wadsley (1953) showed that romanechite has a framework structure built up of Mn octahedra, but he obtained little information on the nature of the Ba-containing tunnels. Recently, Turner and Post (1988) refined the superstructure of romanechite that results from ordering of tunnel Ba and water molecules. Our thermal data, showing evolution of water between 400 and 500 °C, are consistent with such an ordered distribution of tunnel species and with the infrared data of Potter and Rossman (1979). The ordered Ba-H_2O distribution and the relatively small tunnels in romanechite must significantly inhibit the evolution of water upon heating.

The structure of todorokite, and even the validity of the material as a mineral, has been a point of contention in the literature for some time (Burns et al., 1983, 1985; Giovanoli, 1985a, 1985b). Todorokite was assumed to have a layer-like structure (Potter and Rossman, 1979), but based on transmission-electron-microscopy studies, Turner (1982) and Turner and Buseck (1979, 1981) suggested that todorokite has a framework structure. Recently, Post and Bish (1988) confirmed the framework structure of todorokite using Rietveld refinement techniques with X-ray powder-diffraction data. Our thermal data, showing the minor effect of heating todorokite to 500 °C with the simultaneous evolution of most of the water in the structure, strongly support a tunnel structure for todorokite. The large tunnels in todorokite contain more water molecules and fewer tunnel cations than do those in coronadite and romanechite, and the large tunnel size facilitates the evolution of water at lower temperatures in todorokite than in romanechite. The wide temperature range over which water is evolved from todorokite suggests that water molecules are held with a variety of energies in the todorokite tunnels, a concept consistent with Potter and Rossman's (1979) infrared data and Post and Bish's (1988) structural data showing one well-defined water site and several other disordered water sites. There is also evidence that the nature of the tunnel cations affects the total amount of water and the manner in which the water is evolved upon heating. For example, the Cuban todorokite, with the highest tunnel-cation charge (+0.73 per 12 oxygens), retains water to the highest temperature. The behavior of todorokite on heating—including the minor relaxation of the structure and the inclusion of water molecules held with a variety of bond energies—is very similar to that observed for many zeolites such as clinoptilolite (Bish, 1984, 1988). In fact, many properties of these complex tunnel-structure manganese oxides are similar to those of certain zeolites. These manganese oxides have noninterconnected tunnels (as opposed to the generally interconnected tunnels in zeolites) that are infinite in one dimension, and the structures are relatively insensitive to heating to moderate temperatures. They also exhibit cation-exchange phenomena, al-

though their framework charges are generally small, yielding very limited exchange capacities. However, the Mn oxides have added complexity in that they evolve oxygen and undergo major structural transformations as the Mn^{4+} in their structures is reduced upon heating.

Conclusions

The thermal data presented here demonstrate that the complex tunnel-structure manganese oxide minerals coronadite, romanechite, and todorokite all behave in a similar manner when heated. The primary effect of heating these minerals is reduction of Mn^{4+} at high temperatures with concomitant oxygen evolution and structural transformation. None of the minerals is modified significantly below 400 °C, which is consistent with their framework tunnel structures. The amount of water in these minerals is determined by a combination of both structure and tunnel cation. The 3 × 3 tunnels in todorokite accommodate considerably more water than do the 2 × 3 tunnels in romanechite or the 2 × 2 tunnels in coronadite, but water evolution does not appear to have a significant impact on the behavior of any of these structures. Similarly, the tunnel species exert considerable control over the water contents of these minerals but affect the structures in only a minor way. It is apparent, however, that the water molecules occur in crystallographically well-defined sites in romanechite and todorokite (and perhaps coronadite) and persist in all tunnel-structure minerals examined in significant amounts to over 300 °C.

In addition to providing insight into the effects of tunnel cation on the todorokite structure, our Ba- and Sr-exchange data (Table 1) suggest that todorokite (and probably romanechite and hollandite minerals) is not an important cation-exchanging phase. Although neither Ba- nor Sr-exchange was complete, the total tunnel-cation occupancy is too small for todorokite to be a major cation-exchanging mineral. However, the ease with which the tetravalent manganese oxides are reduced upon heating suggests that they may be important in affecting the redox conditions of solutions that come into contact with them. It is these potential redox reactions, in which the Mn is reduced and other species are oxidized, that probably constitute one of the most important aspects of the natural occurrence of manganese oxides. Redox processes at the surfaces of manganese oxides can significantly affect the equilibrium solubility of associated metals (Hem, 1978) and consequently may contribute to the sorption or liberation of metals at the oxide surface.

Acknowledgments

We are grateful to S. J. Chipera for assistance with experiments; to D. T. Vaniman for comments on the manuscript; to H. Allen for editorial corrections to the manuscript; and to C. Francis, Harvard University, and the U.S. National Museum for supplying most of the samples studied. This work was supported by the Nevada Nuclear Waste Storage Investigations Project as part of the Civilian Radioactive Waste Management Program of DOE.

References cited

Appleman, D.E., and Evans, H.T., Jr. (1973) Job 9214: Indexing and least-squares refinement of powder diffraction data. U.S. National Technical Information Service, Document PB2-16188.

Bish, D.L. (1984) Effects of exchangeable cation composition on the thermal expansion/contraction of clinoptilolite. Clays and Clay Minerals, 32, 444–452.

——— (1988) Effects of composition on the dehydration behavior of clinoptilolite and heulandite. In D. Kallo, Ed., Occurrence, properties and utilization of natural zeolites, p. 565–576. Akadémiai Kiadó, Budapest, and D. Reidel, Dordrecht, Netherlands.

Bish, D.L., and Post, J.E. (1984) Thermal behavior of todorokite and romanechite. Geological Society of America Abstracts with Programs, 16, 446.

——— (1985) Rietveld refinement of the crystal structures of todorokite, romanechite, and coronadite. Geological Society of America Abstracts with Programs, 17, 524.

Burns, R.G., and Burns, V.M. (1977) The mineralogy and crystal chemistry of deep-sea manganese nodules, a polymetallic resource of the twenty-first century. Philosophical Transactions of the Royal Society of London, A286, 283–301.

Burns, R.G., Burns, V.M., and Stockman, H.W. (1983) A review of the todorokite-buserite problem: Implications to the mineralogy of marine manganese nodules. American Mineralogist, 68, 972–980.

——— (1985) The todorokite-buserite problem: Further considerations. American Mineralogist, 70, 205–208.

Chen, C.-C., Golden, D.C., and Dixon, J.B. (1986) Transformation of synthetic birnessite to cryptomelane: An electron microscopic study. Clays and Clay Minerals, 34, 565–571.

Dubrawski, J.V., and Ostwald, J. (1987) Thermal transformations in marine manganates. Neues Jahrbuch für Mineralogie Monatshefte, 406–418.

Faulring, G.M., Zwicker, W.K., and Forgeng, W.D. (1960) Thermal transformations and properties of cryptomelane. American Mineralogist, 45, 946–959.

Fleischer, M., and Richmond, W.E. (1943) The manganese oxide minerals: A preliminary report. Economic Geology, 38, 269–286.

Giovanoli, R. (1985a) Layer structures and tunnel structures in manganates. Chemie der Erde, 44, 227–244.

——— (1985b) A review of the todorokite-buserite problem: Implications to the mineralogy of marine manganese nodules: Discussion. American Mineralogist, 70, 202–204.

Golden, D.C., Dixon, J.B., and Chen, C.-C. (1986) Ion exchange, thermal transformations, and oxidizing properties of birnessite. Clays and Clay Minerals, 34, 511–520.

Golden, D.C., Chen, C.-C., and Dixon, J.B. (1987) Transformation of birnessite to buserite, todorokite, and manganite under mild hydrothermal treatment. Clays and Clay Minerals, 35, 271–280.

Gruner, J.W. (1943) The chemical relationship of cryptomelane (psilomelane), hollandite, and coronadite. American Mineralogist, 28, 497–506.

Hem, J.D. (1978) Redox processes at surfaces of manganese oxide and their effects on aqueous metal ions. Chemical Geology, 21, 199–218.

Kulp, J.L., and Perfetti, J.N. (1950) Thermal study of some manganese oxide minerals. Mineralogical Magazine, 29, 239–251.

MacKenzie, R.C., and Berggren, G. (1970) Oxides and hydroxides of higher-valency elements. In R. C. MacKenzie, Ed., Differential thermal analysis, p. 269–302. Academic Press, London.

Post, J.E., and Bish, D.L. (1988) Rietveld refinement of the todorokite structure. American Mineralogist, 73, 861–869.

Post, J.E., Von Dreele, R.B., and Buseck, P.R. (1982) Symmetry and cation displacements in hollandites: Structure refinements of hollandite, cryptomelane, and priderite. Acta Crystallographica, B38, 1056–1065.

Potter, R.M., and Rossman, G.R. (1979) The tetravalent manganese oxides: Identification, hydration, and structural relationships by infrared spectroscopy. American Mineralogist, 64, 1199–1218.

Straczek, J.A., Horen, A., Ross, M., and Warshaw, C.M. (1960) Studies of the manganese oxides: IV. Todorokite. American Mineralogist, 45, 1174–1184.

Turner, S. (1982) A structural study of tunnel manganese oxides by high-resolution transmission electron microscopy. Ph.D. thesis, Arizona State University, Tempe, Arizona.

Turner, S., and Buseck, P.R. (1979) Manganese oxide tunnel structures and their intergrowths. Science, 203, 456–458.

——— (1981) Todorokites: A new family of naturally occurring manganese oxides. Science, 212, 1024–1027.

Turner, S., and Post, J.E. (1988) Refinement of the substructure and superstructure of romanechite. American Mineralogist, 73, 1155–1161.

Wadsley, A.D. (1950) Synthesis of some hydrated manganese minerals. American Mineralogist, 35, 485–499.

——— (1953) The crystal structure of psilomelane, $(Ba,H_2O)_2Mn_5O_{10}$. Acta Crystallographica, 6, 433–438.

Manuscript received April 11, 1988
Manuscript accepted October 5, 1988